Title: Discriminability measures and time-frequency features: An application to vibrissal tactile discrimination

Author: Álvaro G. Pizá Fernando D. Farfán Ana L. Albarracín Gabriel A. Ruiz Carmelo J. Felice

PII: S0165-0270(14)00213-1
DOI: http://dx.doi.org/doi:10.1016/j.jneumeth.2014.06.007
Reference: NSM 6942

To appear in: *Journal of Neuroscience Methods*

Received date: 22-4-2014
Revised date: 4-6-2014
Accepted date: 6-6-2014

Please cite this article as: Pizá ÁG, Farfán FD, Albarracín AL, Ruiz GA, Felice CJ, Discriminability measures and time-frequency features: An application to vibrissal tactile discrimination, *Journal of Neuroscience Methods* (2014), http://dx.doi.org/10.1016/j.jneumeth.2014.06.007

Discriminability measures and time-frequency features: An application to vibrissal tactile discrimination

Álvaro G. Pizá[1,2], Fernando D. Farfán[1,2], Ana L. Albarracín[1,2], Gabriel A. Ruiz[2], and Carmelo J. Felice[1,2]

[1] Instituto Superior de Investigaciones Biológicas (INSIBIO), CONICET – UNT, and Departamento de Bioingeniería, Facultad de Ciencias Exactas y Tecnología, UNT. Av. Independencia 1800, 4000 – San Miguel de Tucumán, Argentina.

[2] Laboratorio de Medios e Interfases (LAMEIN), Universidad Nacional de Tucumán, Argentina.

Phone: (0054)-(381)-4364120

Email addresses:

AGP: piza.ag@gmail.com

FDF: ffarfan@herrera.unt.edu.ar

ALA: anaalbarracin@gmail.com

GAR: gruiz@herrera.unt.edu.ar

CJF: cfelice@herrera.unt.edu.ar

Highlights

- We proposed four discriminability measures to quantify differences of experimental conditions.
- The methods are based on information theory, percentage overlap and divergence between distributions.
- The methods were evaluated on experimental protocols related to vibrissal tactile discrimination.
- The methods indicate the time intervals where sweep conditions have higher probability of being discriminated one from other.
- The methods here proposed can be adapted to many other features of biological responses.

ABSTRACT

BACKGROUND

Often, the first problem that the neuroscientist must face is to determine if a specific stimulus set applied to biological system produces specific, precise and well differentiated responses.

NEW METHOD

In the present study we have proposed four discriminability measures to evaluate the feasibility of differentiating experimental conditions: Information measures based on Information Theory, percentage overlap based on Linacre method, Bhattacharyya distance and univariate standard distance. All discriminability measures were evaluated on experimental protocols related to vibrissal tactile discrimination.

RESULTS

Time-frequency features were extracted from afferent discharges and then, pairwise comparisons were realized by using the proposed discriminability measures. Our results reveal the existence of time-frequency patterns which allows differentiating of sweep conditions from multifiber recordings.

COMPARISON WITH EXISTING METHODS

Currently, statistical methods used to justify significant differences in experimental conditions have rigorous criteria that must be met for correct validation of results. Discriminability measures proposed here are robust and can be adjusted to different experimental conditions (time series, repeated measures, specific variables and other).

CONCLUSIONS

Discriminability measures allowed determining the time intervals where two sweep situations have the highest probability to be differentiated from each other. High discriminability percentages were observed into protraction phase, although to a lesser degree, it were also observed in retraction phase. It was demonstrated that sensibility of discriminability measures are different. This revealing a greater ability to highlight

percentage changes of pairwise comparisons. Finally, the methods here proposed can be adapted to other features of biological responses.

Keywords

Information Theory, discriminability, spectrogram, Texture discrimination, afferent activity, vibrissae.

1. INTRODUCTION

Understanding how neurons represent, process, and manipulate information is one of the main goals of neuroscience (Victor, 2006). Therefore, the nervous system has to interpret what is going on in the real world through the neuronal responses. In short, this means identifying a particular stimulus (or extracting the value of a stimulus parameter) by using the responses of one or more neurons (Dayan and Abbott, 2005). The first problem that the neuroscientist must face is to determine if a specific stimulus set applied to biological system produces specific, precise and well differentiated responses. Often this first exploration is performed through a time-frequency analysis (Victor, 2006).

Time-frequency (or spectrotemporal) analysis is a general exploratory method that is particularly suitable for neural data, both spiking and continuous (Mitra and Pesaran 1999). This analysis allows identifying meaningful statistical structure in spike trains. Its frequent use is due to that neural signal, especially those influenced by external stimuli, are nonstationary (i.e. its statistical properties change along time). Therefore, neural signal is segmented into periods that are sufficiently brief so that within each one, the signals can be assumed stationary. Then, standard spectral analysis applied to each segment can then reveal how the frequency characteristics of a signal evolve over time. Thus, time-frequency analysis provides specific information which can be related to neural encoding of sensory information. For this, a specific stimulus set applied to biological system should produce time-frequency features well differentiated.

The discriminability of neural responses evoked by different stimuli is one of the main indicators of existence of some neural encoding. Discriminability measures have been derived from information theory (Shannon, 1948) and signal-detection theory (Green and Swets, 1974). Information theory has been applied to quantify the amount of information conveyed by neuronal responses (Borst and Theunissen, 1999; Haag and Borst, 1997; Koch et al, 2004; Passaglia and Troy, 2004). Measures of the discriminability of neuronal responses have been applied to estimate the relevant time scale of neuronal coding (Kretzberg et al, 2001; Machens et al, 2001) or to quantify the response reliability (Grewe et al, 2003; Chichilnisky and Rieke, 2005). Both types of reliability measures, i.e. the

theoretical information and the signal-detection ones, shed light on the accuracy with which a sensory system encodes stimuli (Grewe et al, 2007).

In this paper we have proposed four discriminability measures, one of which is based on Information Theory. The second proposed method is based on estimates of percentage overlap between normal distributions proposed by Linacre (1996). The third and fourth measures are Bhattacharyya and Univariate standard distances which are measures of divergence between two distributions (Bhattacharyya, 1943; Flury and Riedwyl, 1986). All discriminability measures were applied to texture discrimination problem in the rat vibrissal system (Albarracín et al, 2006).

It is well known that rats acquire sensory information by actively moving their vibrissae, and a neural code is manifested at different levels of the sensory system (Arabzadeh et al. 2006; Diamond et al 2008; Farfán et al, 2013). Particularly, Wolfe et al (2008) found that when a vibrissa sweep over a rough surface, it experiences changes in its trajectory characterized by irregular and skipping motions (known as slip-stick events) and thus producing a pattern of slip-stick events which would be related to surface features like the size of grains and the distance between them. Farfán et al. (2013) showed that it is possible to identify electrophysiological events evoked by mechanical slip-tick events by exploring the afferent activity recordings, and that these would allow discrimination of rough surfaces at peripheral level.

Here, we analyzed the afferent discharge from a deep vibrissal nerve when the vibrissa sweeps materials (wood, metal, acrylic, sandpaper) having different textures. Just like Albarracín et al (2006), here we also consider the change of slip-resistance of vibrissa over surfaces as a way to improve the tactile information acquisition. Time-frequency features from afferent recordings were obtained for each experimental condition (sweep over different surfaces). Then, pairwise comparisons were realized by using the proposed discriminability measures. We demonstrated that experimental sweep conditions can be discriminated with time-frequency features and discriminability measures.

2. MATERIALS AND METHODS

2.1. PROCEDURES

Five Wistar adult rats (300 g – 350 g) were used in our experiments. They were anesthetized with urethane (1.5 g/Kg) and their temperature was maintained at 37° by a servo-controlled heating pad. Surgery consisted of exposing the infraorbital nerve as well as the two branches of the facial nerve (buccal and upper marginal mandibular) on the right side. The motor branches were dissected and transected proximally to avoid possible motor influences on the sensorial pathway. The stimulation electrodes were placed on their distal stumps to produce the contraction of the mystacial muscles. The deep vibrissal nerve innervating a vibrissal follicle (Gamma vibrissa) was identified with a high magnification dissecting microscope. The dissected nerve was also transected proximally and this action allowed eliminating discharges arriving from higher level of the sensorial pathway. To make sure that the nerve transection did not affect the functionality of the vibrissal nerve during our recording time, we have tested the reduction in the nerve afferent activity throughout the time (data not shown). We concluded that the activity starts decreasing approximately over 1 hour after the nerve transaction, so we never exceeded this space of time in our experiments. We used a bipolar electrode (insulated silver wire, 0.2mm diameter) to record the multifiber afferent discharge of the vibrissal nerve selected. The recording electrodes as well as the nerves were immersed in a mineral oil bath during all recording.

All these procedures were carry out in accordance with the recommendations of the Guide for the Care and Use of Laboratory Animals (National Research Council, NRC).

2.2. RECORDING OF THE VIBRISSA ELECTRICAL ACTIVITY

In this study we have recorded the multifiber activity of the Gamma vibrissal nerve while the vibrissa was sweeping surfaces of different textures. The experimental protocol used in this paper has been previously described in detail by Albarracín et al. (2006) and Farfán et al. (2011, 2013). The procedures are briefly described below.

Vibrissa movements were induced by electrical stimulation of facial motor nerve (VII). Square-wave pulses (30 μs, 7V supramaximal[1], 5 Hz) simulated vibrissal whisking at its natural frequency (a diagram of experimental set up is shown in Fig. 1B).

Nerve activity was recorded and digitized at 20 kHz (sampling rate, Fs) during a 100 ms window following onset of each cycle of whisker movement with a Digidata 1322A (Axon Instruments). Fifty whisker movement cycles were obtained for each surface, and an additional 50 cycles were recorded while whisker moved unobstructed in air (control).

Four slip-resistance levels were presented for each surface by mounting the surface at different distances from the whisker base. A minimal slip-resistance level was presented by placing the surface at a maximal distance from the whisker base so that the tip just barely contacted the surface throughout the entire movement cycle (slip-resistance 1). Increased slip-resistance levels were presented by moving the surface 3, 6 or 9 mm closer to the whisker base (slip-resistance 2, 3 and 4, respectively) (Albarracín et al, 2006).

Movements of the Gamma whisker were recorded simultaneously with nerve activity using a custom-made photoresistive sensor (Fig. 1B). The frequency response of the sensor was maximal in the range 0-100 Hz, enabling direct identification of the protraction and retraction phases of the movement cycle (Dürig et al. 2009).

2.3. ROUGH SURFACES

The swept surfaces used in this paper were surfaces with different textures: wood, metal, acrylic and sandpaper P1000 (Fig. 1A). Three surfaces (wood, metal and acrylic) were polished using the same grade sandpaper P1000. This procedure allowed us to obtain surfaces with similar roughness and different textures.

Surface texture is not a measurable quantity; it is not possible to assign a unique "texture" value to every different surface. However, it is possible to measure some of the intrinsic characteristics, or parameters, of surface texture. Thus, we measured the surfaces roughness by using a Hommel Tester T1000 (HommelWerke, www.hommel-etamic.de) and we used the Ra parameter (arithmetical deviation of the assessed profile) as a

[1] A supramaximal stimulation should simultaneously depolarise all of nerve fibres within the nerve.It is 20-50% above a stimulation that causes maximal response.

roughness estimation (International Standards BS.1134 and ISO 468). Ra values are shown in Fig. 1A.

FIGURE 1

2.4. DIGITAL PROCESSING AND STATISTICS

2.4.1. SPECTROGRAM VIA SHORT-TIME FOURIER TRANSFORM

One commonly used time−frequency representation is the short-time Fourier transform (Qian, 2002), defined as:

$$STFT_x(\tau, f) = \int_{-\infty}^{\infty} x(t) \times \omega(t-\tau) \times e^{-j\times 2\pi \times f \times t} df = \int_{-\infty}^{\infty} x(t) \times \omega^*_{t,f}(t) dt \quad (1)$$

Where $\omega^*_{t,f}(t) = \omega(t-\tau) \times e^{-2\pi \times f \times t}$. *STFT* analyses the signal $x(t)$ through a short-time window $\omega(t) = x(t) \times \omega(t-\tau)$, and then a Fourier transform is performed on this product using complex exponential basis functions. The square modulus of *STFT* is referred to as the spectrogram (Zhan et al, 2006).

$$SPEC_x(\tau, f) = |STFT_x(\tau, f)|^2 \quad (2)$$

Thus, the spectrogram of each multifiber activity recording was calculated by using following parameters: Hamming window length (HWL) of 200 samples, overlap between segments of 97.5% (195 samples), FFT length of 200 (Fig. 2A). Time-frequency diagrams were reduced to time interval from 5 to 95 ms because windowing used. Thus, frequency resolution of spectrogram results 100 Hz (sampling rate/HWL).

2.4.2. MAXIMUM ENERGY FREQUENCY COMPONENTS VS TIME

Maximum energy components into frequency range of 10 to 1000 Hz were obtained for each spectrogram along time. Thus, the spectrogram information, provided in three dimensions (frequency, amplitude and time), is reduced to a time series (frequency of

maximum energy values vs time). Then, fifty time series represents one experimental situation (Fig. 2B).

2.4.3. DISCRIMINABILITY MEASURES

Discriminability between all possible pairs of experimental situations were measured using four methods: information measures using theory information (Shannon, 1948; Cover and Thomas, 1991; Farfán et al, 2013), overlap percentage estimations (Linacre, 1986), Bhattacharyya distance (Bhattacharyya, 1943) and univariate standard distance (Flury and Riedwyl, 1986).

2.4.4. INFORMATION MEASURES (I)

The information that time-frequency features from afferent activity convey about the stimulus can be quantified by Shannon's mutual information formula (Cover and Thomas, 1991), abbreviated hereafter as information:

$$I = \sum P(r) \times P(s|r) \times \log_2 (P(s|r) / P(s)) \quad (3)$$

Where *P(s)* is the probability of presentation of roughness stimulus *s*, *P(s|r)* is the posterior probability of *s* given observation of *r*, and *P(r)* is the probability of *r* unconditional on the stimulus. Information determines the maximum amount of knowledge (the upper bound of information) available to an observer who knows the posterior probabilities *P(s|r)* and uses them to read off the signals available in a single observation of a spike train (Rieke et al., 1997). Details about probability distribution estimations of eq. 3 are described by Farfán et al, 2013.

Here, the information was obtained for each pair of experimental situation along time. In short, *I* values (eq. 3) were obtained as follow:

1. First, the frequency diagrams (or histograms) for each time are determined. For each experimental situation, the number of occurrences of *r* is obtained. Response *r* is the maximum energy component into frequency range of 10 to 1000 Hz (Fig. 2C).

2. Determination of the joint probability distribution, *P(s,r)* (Fig. 2D).

3. Determination of the *P(r)* and *P(s)* probability distributions. The probability of obtaining a response *r*, regardless of whether stimulus *s* did or not occur, is called the marginal probability, and it can be calculated by the sum of joint probabilities for a given response *r*.

4. Determination of conditional probability distribution *P(s|r)*.

5. Determination of the amount of information. After obtaining all probability distributions, it is possible to obtain the mutual information using eq. 3.

The stimulus-response probabilities in the above formula (eq. 3) are not known a priori and must be estimated empirically from a limited number, N, of experimental trials for each unique stimulus. In our data set, N was 50. Limited sampling of response probabilities can lead to an upward bias in the estimate of information (Optican et al. 1991; Panzeri and Treves 1996; Golomb et al. 1997; Victor 2000; Paninski 2003). We used a number of bias-correction procedures (Panzeri and Treves, 1996). Because they all have almost identical results, we present only results based on the quadratic extrapolation correction procedure. This bias correction procedure assumes that the bias can be accurately approximated as second order expansions in $1/N_{tr}^{tot}$ (where N_{tr}^{tot} is the number of trials), that is:

$$bias = a/N_{tr}^{tot} + b/\left(N_{tr}^{tot}\right)^2 \qquad (4)$$

Where *a* and *b* are free parameters that depend on the stimulus-response probabilities, and are estimated by re-computing the information from fractions of the trials as follows. The dataset is first broken into two random partitions and the information quantities are computed for each sub-partition individually: the average of the two partitions provides an estimate corresponding to half of the trials. Similarly, by breaking the data into four random partitions, it is possible to obtain estimates corresponding to a fourth of the trials. Finally, *a* and *b* are extrapolated as parameters of the parabolic function passing through the $N_{tr}^{tot}/2$ and $N_{tr}^{tot}/4$ estimates (Magri et al, 2009).

FIGURE 2

2.4.4.1. PERCENTAGE OVERLAP BETWEEN NORMAL DISTRIBUTIONS (LDF)

Discriminability of two experimental situations was estimated by measuring the percentage overlap between distributions of maximum energy components. Time series mean and standard deviation of fifty time series (Fig. 2B) were calculated according to grouped data theory. For this, a frequency distribution histogram (FDH) most be created (Fig. 2C). The number of histogram bins was ten, while histogram bin size is 100 Hz (10 to 1000 Hz, in steps of 100 Hz). Then, mean and standard deviation are calculated as follows:

$$\hat{\mu} = \left(\sum_{i=1}^{M} x_i \times h_i \right) / M \tag{5}$$

$$\hat{\sigma} = \sqrt{\left(\sum_{i=1}^{M} \left(x_i - \hat{\mu} \right)^2 \times h_i \right) / (M - 1)} \tag{6}$$

Where, $\hat{\mu}$ and $\hat{\sigma}$ are estimates of mean and standard deviation, M is class number (number of histogram bins), x_i is the mean value of *i-th* class, and h_i is the number of elements of each bin. Therefore, each experimental situation is represented by a $\hat{\mu}(t)$ time series with its corresponding $\hat{\sigma}(t)$.

To compare the experimental conditions we have estimated the overlap percentage along the time axis. This percentage was proposed by Linacre (1996). Next, we state the major steps of the procedure:

The percentage by which each sample of $f_2(x)$ overlaps the $f_1(x)$ can be estimated by calculating the area under the $f_1(x)$ distribution from $-\infty$ to x_1 plus the area under $f_2(x)$ distribution from x_1 to x_2 plus the area under $f_1(x)$ from x_2 to ∞ (Fig. 3). Written in symbolic form:

$$A_{overlap} = \int_{-\infty}^{x1} f_1(x)dx + \int_{x1}^{x2} f_2(x)dx + \int_{x2}^{\infty} f_1(x)dx \tag{7}$$

Where:

$A_{overlap}$: is the overlap area of function f_2 on f_1.

$f_1(x)$ and $f_2(x)$ are functions of normal distribution. f_1 and f_2 parameters are μ_1, μ_2, σ_1 and σ_2, corresponding to the averages and standard deviations.

x_1 and x_2 are points of intersection between $f_1(x)$ and $f_2(x)$.

FIGURE 3

Fig. 3 shows the overlap area ($A_{overlap}$) obtained from eq. 7. A nomogram for the relationship of averages, variances and overlap percentage, can be found. We suppose that:

$$A_{overlap} / A_{f1} = K \times 100 \tag{8}$$

Where $A_{overlap}$ is the overlap area and A_{f1} is the area under f_1 distribution.

If we consider A_{f1}=constant, then $A_{overlap}$ can be written as a function of $|\mu_2 - \mu_1|/\sigma_1$ and σ_2/σ_1 (Linacre, 1996). Fig. 4 shows the resulting nomogram.

FIGURE 4

Finally, a relationship between overlap percentage and variables Z and W can be established ($f[z,w]=K$).

$$\begin{aligned} p(z,w) = {} & \frac{1}{2}\times\left(1+Erf\times\left[\left(-z+\sqrt{w^2\times\left(z^2+2\times\left(-1+w^2\right)\times\log(w)\right)}\right)/\sqrt{2}\times\left(1-w^2\right)\right]\right)+ \\ & \frac{1}{2}\times Erf\times\left[\left(z\times w^2+\sqrt{w^2\times\left(z^2+2\times\left(-1+w^2\right)\times\log(w)\right)}\right)/\left(\sqrt{2}\times\left(-w-w^3\right)\right)\right]+ \\ & \frac{1}{2}\times Erf\times\left[\left(-z\times w^2+\sqrt{w^2\times\left(z^2+2\times\left(-1+w^2\right)\times\log(w)\right)}\right)/\left(\sqrt{2}\times\left(-w-w^3\right)\right)\right]+ \\ & \frac{1}{2}\times\left(1+Erf\times\left[\left(z+\sqrt{w^2\times\left(z^2+2\times\left(-1+w^2\right)\times\log(w)\right)}\right)/\sqrt{2}\times\left(1-w^2\right)\right]\right) \end{aligned} \tag{9}$$

Where $Erf[X]$ is the error function for each element of X. The error function is defined as:

$$Erf[X] = \left(2/\sqrt{\pi}\right)\times\int_0^X e^{-t^2}\,dt \tag{10}$$

In short, at each instant of time a standardized absolute distance between the means ($|\mu_A - \mu_B|/\sigma_A$) and the ratio of the standard deviations (σ_B/σ_A) are calculated. Where μ_A

and μ_B are Fmax averages at time t_i of A and B situations. σ_A and σ_B are the standard deviations of A and B situations. Thus, this method allows to discover the expected percentage by which each sample distribution overlaps the other ($A_{overlap}$). Finally, a discriminability measurement between two experimental situations will be given by:

$$LDF = 1 - A_{overlap} \tag{11}$$

Where *LDF* is the Linacre discriminability factor.

2.4.4.2. BHATTACHARYYA DISTANCE (D_B)

The Bhattacharyya distance is a measure of divergence between two distributions (Bhattacharyya, 1943). In its simplest formulation, the Bhattacharyya distance between two classes under approximately normal distributions can be calculated by extracting the mean and variances of two separate distributions or classes.

$$D_B(p,q) = (1/4) \times \ln\left[(1/4) \times \left(\sigma_p^2 / \sigma_q^2 + \sigma_q^2 / \sigma_p^2 + 2\right)\right] + (1/4) \times \left[\left(\mu_p - \mu_q\right)^2 / \left(\sigma_p^2 + \sigma_q^2\right)\right] \tag{12}$$

Where, $D_B(p,q)$ is the Bhattacharyya distance between p and q distributions or classes, σ_p is the variance of the *p-th* distribution, μ_p is the mean of the *p-th* distribution, and p, q are two different distributions.

Here, D_B (*sitA, SitB*) was calculate along time. μ and σ were obtained by using eq. 5 and 6, respectively.

2.4.4.3.UNIVARIATE STANDARD DISTANCE (D)

Comparing two sample means μ_p and σ_p is one of the basic statistical problems. Here we purposed a simple formulation given by Flury and Riedwyl (1986) which consists in comparing two sample means in terms of the standard distance.

$$D = \left|\mu_p - \mu_q\right| / s \tag{13}$$

$$s^2 = \left(s_p^2 - s_q^2\right) / \left(N - 2\right) \tag{14}$$

Where s^2 is the pooled variance of both samples (eq. 14). It can be interpreted as mean difference in units of the standard deviation. Here, D was calculated along time. μ, and σ were obtained by using eq. 5 and 6, respectively.

3. RESULTS

The afferent discharge recorded here is the average electrical activity of about 200 myelinated axons (Albarracín et al, 2006; Farfán et al, 2013) and not all of those fibers have the same firing patterns. Fig 5A shows the multifiber recordings belonging to Gamma vibrissa innervation recorded during a control sweep, and its corresponding vibrissal displacement. The whisker displacements and evoked afferent activity were recorded simultaneously at the same sampling frequency. From displacement recordings is possible to identify the protraction, retraction and resting phases. In this last phase the Gamma vibrissa remains in its natural position in order to complete a 100 ms period (sweep frequency 10 Hz). In afferent recording is possible to observe a stimulus artifact at $t = 2$ *ms* and an artifact generated by the volume conduction of EMG at $t = 4$ *ms*.

Fig. 5B shows five afferent recordings in different sweep situations at slip-resistance 1. Amplitude of afferent discharge does not vary significantly for control and sweep on wood, metal and acrylic. However, an afferent discharge of greater amplitude are observed when the vibrissa to sweep over sandpaper. This particularity is due to high roughness values of sandpaper (4.31 μm) compared to other sweep surfaces (acrylic 0.30 μm, metal 0.11 μm and wood 2.52 μm). At slip-resistance 2 the amplitude of afferent discharges increased (Fig. 5C), revealing a dependence with surfaces roughness. Thus, one can observe that when sweep the vibrissa on wood evoke higher discharges than sweep on acrylic. The sweeps on sandpaper evoked highest afferent discharges. Similar results are observed when slip-resistence increase to level 4 (Fig. 5D).

Spectrogram was obtained for each afferent activity recording, and maximum energy components, into frequency range of 10 to 1000 Hz, were determined along time. Thus, fifty time series (Fmax vs time) were obtained for each sweep situation. The mean and standard deviations of Fmax along time from two situations are shown in Fig. 6. A qualitative observation reveals that difference between Fmax means varies according to

slip-resistance levels into protraction and retraction phases (10 - 50 ms). Such differences between means are quantitatively estimated by overlap degree between the shaded areas.

FIGURE 5

FIGURE 6

Fig. 7A shows means and standard deviations of Fmax along time belonging to sweep over wood and acrylic at slip-resistance 4. Discriminability measures between sweep situations are shown in Fig.7B. All discriminability measures lead to similar results. These show quantitative differences between sweep situations into protraction and retraction phases of vibrissal sweep. All discriminability measures provide quantitative values with different units (e.g. I value is measured in bits, while LDF value is measured in percentages). To compare the different discriminability measures, these were standardized to their corresponding means and standard deviations values into resting state phase. Thereby it is possible quantifying the discriminability between sweep situations according to the percentage increase respect to its mean value into resting state phase (Discriminability Factor normalized, DFn).

Fig. 7C shows the four standardized discriminability measures in percentage units (percentage increase respect to discriminability measures into resting state phase). It is possible to observe that standardized Bhattarcharyya distance (D_Bn) has greater percentage changes into protraction phase (10 a 30 ms).

FIGURE 7

Standardized discriminability measures for sweep situations of Fig. 6 are displayed in Fig. 8. Sweep on wood vs acrylic situations do not show significant increases in their discriminability measures at slip-resistance level 1 (Fig. 8A, left). On the other hand, sweep wood vs metal and wood vs sandpaper situations, show significant increases in their discriminability measures, mainly into protraction phase. An increased of slip-resistance to level 2 causes an discriminability increase of sweep wood vs acrylic situations into temporal range from 18 to 30 ms (Fig. 8B, left). Standardized information measure (In) reflects this particularity. An increase of discriminability measures at 20 ms is observed for sweep wood vs metal situations (Fig. 8B, middle), while a decrease at 20 ms is observed for sweep wood vs sandpaper situations (LDFn, D_Bn y Dn) and an increase at 40 ms (D_Bn).

At slip-resistance 4, sweep wood vs acrylic situations produces a significant increase in their discriminability measures (reflected mainly by LDFn, D_Bn and Dn factors) into temporal range from 20 to 35 ms (Fig. 8C, left), while sweep on wood vs metal situations are not discriminable from each other. (Fig. 8C, middle).

FIGURE 8

4. DISCUSSION

In the present study we have proposed different discriminability measures to evaluate the feasibility of differentiating sweep situations with time-frequency features extracted from afferent activity recordings. Our results reveal the existence of time-frequency patterns which allows differentiating of sweep situations from multifiber recordings. All discriminability measures indicate the time intervals where two sweep situations have higher probability of being discriminated one from other. However, the sensitivity of these indicators is different. Sensitivity refers to percentage changes of indicator respect to its average value in a reference phase (here, reference phase is the resting state). In Fig. 8 is observed that DBn factor is more sensitive than other factors because the percentage changes are larger (solid orange lines). These differences in sensitivity of discriminability measures can improve and highlight areas, or time intervals, where the time-frequency features reveal significant changes. Thus, a more comprehensive analysis of neural encode involved in coding of sensorial information can be better planned.

The lower sensitivity was observed in information measures, I_n (Fig 8, solid black lines). Similar results were observed by Grewe et al (2007), who argued that information measures based on Information Theory are usually applied to evaluate a system's encoding capabilities while signal-detection measures are commonly used to asses the decoder's side of neuronal information processing. Increased response reliability, however, increases the SNR, leads to an increased information capacity and, in parallel, increases response discriminability in the signal-detection task (Grewe et al, 2007). Thus, all discriminability measures proposed here can be employed to tackle the problem of coding performance since they depend similarly on response quality.

Information theory measures the statistical significance of how neural responses vary with different stimuli (Borst and Theunissen, 1999). That is, it determines how much information about stimulus parameter values is contained in neural responses. If stimulus A yields a mean response R_A and stimulus B yields R_B, information in the response could be measured as the difference between R_A and R_B. However, two experimental situations with the same differential response ($R_A - R_B$) may have different variability in their responses. Then the information obtained is greater for the experimental situation with less variability. If response variability is described by the variance, then neuronal information can be described by Linacre discriminability factor, Bhattacharyya distance or Univariate standard distance. However, this is rigorously correct only if the distribution of response probabilities given particular stimulus conditions (conditional probability distribution) is completely specified by their mean and variance, as for Gaussian distributions (Borst and Theunissen, 1999).

The use of information as a statistical measure of significance is an extension of this process. Information theory allows to consider not only response variance, but exact conditional probability distributions. Here, we have estimated conditional probabilities of stimuli *s* (sweep situations) given observation of *r* (time-frequency features), $P(s|r)$, and then we have used the information theory to calculate a distance between two experimental situations. Although this method does not require any Gaussian distribution condition, it is very sensitive to overestimations of information values due to limited sampling of response probabilities (Panzeri and Treves, 1996). Here, we used a number of bias-correction procedures to solve these overestimation problems. Finally, the information measures allowed us to validate other discriminability measures.

4.1. VIBRISSAL TACTILE DISCRIMINATION

It is well known that the rats distinguish surfaces with different roughness through its vibrissal system (Guic-Robles et al, 1989; Carvell and Simons, 1990, 1995), and that there are specific discharge patterns at peripheral level when rats sweep their vibrissae over rough surfaces (Albarracín et al, 2006; Farfán et al, 2011, 2013). Many researches have proposed different mechanisms of transduction and neural encoding of tactile information, however one of the most accepted is the one proposed by Wolfe et al (2008), who found

that when whiskers were moving along the texture, their trajectory was characterized by an irregular, skipping motion: the whisker tip tended to get fixed in place ("stick"), before bending and springing loose ("slip") only to get stuck again. A slip-stick event was a jump in speed and acceleration; the two quantities covaried. Thus, a pattern of slip-stick events would be set by surface features like the size of grains and the distance between them (Diamond et al. 2008; Farfán et al, 2013). Follicular receptors would respond to the most prominent features of the vibrissal movement – the high velocity jumps over texture grains– giving rise to the texture neural code (Arabzadeh et al. 2005; Shoykhet et al. 2000; Ito 1985).

Farfán et al (2013) hypothesized that the follicular receptors transform the mechanical events (slip-tick) to electrical activity (spikes) that would travel through multiple axons (infraorbital nerve) to higher levels. Thus, it is possible to identify electrophysiological events evoked by mechanical slip-tick events by exploring the afferent activity recordings. Here, we explored the existence of time-frequency information which could be related to tactile neural encoding. Preliminary investigations revealed the existence of amplitude and frequency features in afferent activity through which it was possible to discriminate surfaces with different textures (Albarracín et al, 2006). Discriminability measures proposed here reveal time-frequency features along time which could be related to the neural encoding of tactile information.

It is possible to ensure that sweep on wood vs acrylic can not be differentiated from each other by analyzing the time-frequency features at slip-resistance 1 (Fig. 8A). However, these situations can be differentiated around 20 ms at slip-resistance 2 (Fig. 8B). This observation is given by the percentage increase of Information values (bits) with respect to resting state. Sweep on wood vs acrylic can be discriminated from each other into protraction phase (from 10 to 30 ms) at slip-resistance 4 because to percentage increase of all proposed discriminability measures. DBn factor had the greatest percentage changes (Fig. 8C). These results partially agree with those obtained by Albarracin et al, 2006. Discriminability between experimental situations may be due to possible temporal patterns in afferent discharge (electrophysiological events) which encode texture features of sweep surfaces (Farfán et al, 2013).

4.2. LIMITATIONS OF DISCRIMINABILITY MEASURES

The information measures of eq. 3 can be extended to a situation with many stimulus conditions $\{s_A, s_B, s_C, \ldots\}$ to measure how the distribution of responses to any particular stimulus condition 'x' is different from all other conditional distributions that can be obtained. This is done by comparing the conditional probability $P(s_X|r)$ to the unconditional probability $P(r)$ (the probability of the response under any stimulus condition) (Borst and Theunissen, 1999). Discriminability measures proposed here can not be expanded to more than two experimental situations by using the formulations given in eq. 11, 12 and 13. This important limitation can be avoided by using other methods to measure distance among experimental situations, such as Mahalanobis distance (Mahalanobis, 1936) and others.

On the other hand, discriminability measures that involve means and variances in their formulations require the normality condition of distributions of response probabilities. However, the central limit theorem of probability theory states that, given certain conditions, the arithmetic mean of a sufficiently large number of samples of independent random variables will be approximately normally distributed (Rice, 1995). In other words, discriminability measures proposed here can be used in experimental protocols where a significant amount of samples have been extracted.

5. CONCLUSION

We have proposed four discriminability measures which have been implemented to investigate the texture discrimination through time-frequency features of afferent recordings from vibrissal nerve. Discriminability measures allowed to determine the time intervals where two sweep situations have the highest probability to be differentiated from each other. Simultaneously, these allow quantifying the discriminability degree according to percentage changes respect to a stationary state (resting state). High discriminability percentages were observed into protraction phase, although to a lesser degree, were also observed in retraction phase. It was possible to quantify the slip-resistance effect on ability of sweep situations discrimination via time-frequency features. High discriminability percentages were achieved at low slip-resistance level for specific pairwise comparisons,

while others were best discriminated at high slip-resistance level. This suggests that slip-resistance would be a possible behavioral strategy for rough surfaces discrimination.

Finally, it was demonstrated that sensibility of three discriminability measures (LDFn, DBn and Dn) are different of information measurement (In via Information Theory). This revealing a greater ability to highlight percentage changes of pairwise comparisons.

ACKNOWLEDGEMENTS

This work has been supported by grants from Agencia Nacional de Promoción Científica y Tecnológica (ANPCYT); Consejo Nacional de Investigaciones Científicas y Técnicas (CONICET), and Consejo de Investigaciones de la Universidad Nacional de Tucumán (CIUNT), as well as with Institutional funds from Instituto Superior de Investigaciones Biológicas (INSIBIO).

REFERENCES

Albarracín AL, Farfán FD, Felice CJ and Décima EE (2006) Texture discrimination and multi-unit recording in the rat vibrissal nerve. BMC Neuroscience 7, 42.

Arabzadeh E, Panzeri S and Diamond ME (2006) Deciphering the spike train of a sensory neuron: counts and temporal patterns in the rat whisker pathway. The Journal of Neuroscience 26 (36): 9216–9226.

Arabzadeh E, Zorzin E and Diamond ME (2005) Neuronal encoding of texture in the whisker sensory pathway. PLoS Biology 3: e17.

Bhattacharyya A (1943) On a measure of divergence between two statistical populations defined by their probability distributions. Bulletin of the Calcutta Mathematical Society 35: 99–109.

Borst A and Theunissen FE (1999) Information theory and neural coding. Nature Neuroscience 1 (11): 947 – 957.

Carvell GE and Simons DJ (1990) Biometric analyses of vibrissal tactile discrimination in the rat. Journal Neuroscience 10: 2638 – 48.

Carvell GE and Simons DJ (1995) Task and Subject-Related differences in sensorimotor behavior during active touch. Somatosensory Motor Research 12: 1 – 9.

Chichilnisky EJ and Rieke F (2005) Detection Sensitivity and Temporal Resolution of Visual Signals near Absolute Threshold in the Salamander Retina. Journal of Neuroscience 25: 318–330.

Cover TM and Thomas JA (1991) Elements of information theory. New York: Wiley.

Dürig F, Albarracín AL, Farfán FD and Felice CJ (2009) Design and construction of a photoresistive sensor for monitoring the rat vibrissal displacement. Journal of Neuroscience Methods 80 (1): 71–76.

Dayan P and Abbott LF (2005) Theoretical Neuroscience: Computational and Mathematical Modeling of Neural Systems. The MIT Press.

Diamond ME, von Heimendahl M and Arabzadeh E (2008) Whisker-mediated texture discrimination. PLoS Biology 6 (8): e220.

Farfán FD, Albarracín AL and Felice CJ (2011) Electrophysiological characterization of texture information slip-resistance dependent in the rat vibrissal nerve. BMC Neuroscience 12, 32.

Farfán FD, AL Albarracín and CJ Felice (2013) Neural encoding schemes of tactile information in afferent activity of the vibrissal system. Journal of Computational Neuroscience 34: 89–101.

Flury BK and Riedwyl H (1986) Standard distance in univariate and multivariate analysis. The American Statistician 40(3): 249-251.

Golomb D, Hertz J, Panzeri S, Treves A, Richmond B (1997) How well can we estimate the information carried in neuronal responses from limited samples? Neural Comput 9: 649-665.

Green DM and Swets JA (1974) Signal detection theory and psychophysics. Huntington, New York: Robert Krieger Publ. Comp.

Grewe J, Kretzberg J, Warzecha AK, Egelhaaf M (2003) Impact of Photon Noise on the Reliability of a Motion-Sensitive Neuron in the Fly's Visual System. Journal Neuroscience 23: 10776–10783.

Grewe J, Weckström M, Egelhaaf M and Warzecha A-K (2007) Information and Discriminability as Measures of Reliability of Sensory Coding. PLoS ONE 2 (12): e1328.

Guic-Robles E, Valdivieso C and Guajardo G (1989) Rats can learn a roughness discrimination using only their vibrissal system. Behavioural Brain Research 31 (3): 285 – 289.

Haag J and Borst A (1997) Encoding of visual motion information and reliability in spiking and graded potential neurons. Journal Neuroscience 17: 4809–4819.

Ito M (1985) Processing of vibrissa sensory information within the rat neocortex. Journal of Neurophysiology 54: 479–490.

Koch K, McLean J, Berry M, Sterling P, Balasubramanian V and Freed MA (2004) Efficiency of information transmission by retinal ganglion cells. Curr Biol 14: 1523–1530.

Kretzberg J, Warzecha AK, Egelhaaf M (2001) Neural coding with graded membrane potential changes and spikes. Journal of Computational Neuroscience 11: 153–164.

Linacre JM (1996) Overlapping Normal Distributions. Rasch Measurement Transactions 10 (1): 487 - 488.

Machens CK, Stemmler MB, Prinz P, Krahe R, Ronacher B, Herz AV (2001) Representation of acoustic communication signals by insect auditory receptor neurons. Journal Neuroscience 21: 3215–3227.

Magri C, Whittingstall K, Singh V, Logothetis NK, Panzeri S (2009) A toolbox for the fast information analysis of multiple-site LFP, EEG and spike train recordings. BMC Neuroscience 10(1):81.

Mahalanobis PC (1936) On the generalised distance in statistics. Proceedings of the National Institute of Sciences of India 2 (1): 49–55.

Mitra PP and Pesaran B (1999) Analysis of dynamic brain imaging data. Biophysical Journal 76: 691–708.

Optican LM, Gawne TJ, Richmond BJ, Joseph PJ (1991) Unbiased measures of transmitted information and channel capacity from multivariate neuronal data. Biol Cybern 65: 305-310.

Paninski L (2003) Convergence properties of three spike-triggered analysis techniques. Network 14: 437-464.

Panzeri S and Treves A (1996) Analytical estimates of limited sampling biases in different information measures. Network 7: 87-107.

Passaglia CL and Troy JB (2004) Information transmission rates of cat retinal ganglion cells. Journal Neurophysiology 91: 1217–1229.

Qian S (2002) Introduction to time–frequency and wavelet transforms. Prentice Hall PTR, New Jersey.

Reike F, Warland D, De Ruyter van Steveninck R, and Bialek W (1997) Spikes: Exploring the Neural Code. Cambridge, MA: MIT Press.

Rice J (1995) Mathematical Statistics and Data Analysis (Second ed.). Duxbury Press.

Shannon CE (1948) A Mathmatical Theory of Communication. The Bell System Technical Journal 27: 379–423.

Shoykhet M, Doherty D and Simons D (2000) Coding of deflection velocity and amplitude by whisker primary afferent neurons: implications for higher level processing. Somatosensensory Motor Research 17: 171–180.

Victor JD (2000) Asymptotic bias in information estimates and the exponential (Bell) polynomials. Neural Comput 12: 2797-2804.

Victor JD (2006) Approaches to Information-Theoretic Analysis of Neural Activity. Biological Theory 1 (3): 302–316.

Wolfe J, Hill DN, Pahlavan S, Drew PJ, Kleinfeld D and Feldman DE (2008) Texture coding in the rat whisker system: slip-stick versus differential resonance. PLoS Biology 6 (8): e215.

Zhan Y, Halliday D, Jiang P, Liu X and Feng J (2006) Detecting time-dependent coherence between non-stationary electrophysiological signals – A combined statistical and time–frequency approach. Journal of Neuroscience Methods 156 (1–2): 322-332.

FIGURE LEGENDS

Fig. 1 Experimental set up and stimuli set. (A) It shows how the facial nerve must be stimulated for producing the artificial movement of the vibrissa, and the methodology used to obtain the recordings of the electrical activity in the deep vibrissal nerve (modified from Albarracín et al. (2006). (B) Surfaces Pictures. Photographs of the surfaces used in this paper.

Fig. 2 Time-frequency features from spectrograms of afferent recordings. (A) Fifty spectrograms were obtained from fifty afferent recordings for one experimental situation. (B) Maximum energy components into frequency range of 10 to 1000 Hz were obtained for each spectrogram along time. (C) For each Δt (200 samples = 5 ms), frequency diagrams (or histograms) was determined. (D) For each Δt, joint probability distributions were determined.

Fig. 3 Overlap percentage between two normal distributions. (A) Two distributions whose means are equal and $\sigma_1 < \sigma_2$. The points of intersection between f_1 and f_2 are x_1 and x_2. (B) The means are different ($\mu_1 < \mu_2$) and standard deviations are different. The region shaded in both figures represents the overlap area between the distributions ($A_{overlap}$).

Fig. 4 Percent of one normal distribution overlapping another ($p\%$). Z is the distance between means $|\mu_2 - \mu_1|/\sigma_1$, and W is standard deviation ratio σ_2/σ_1.

Fig. 5 Afferent discharges. (A) Displacement and afferent activity recordings from Gamma vibrissa acquired during a control sweep. The displacement recordings were acquired by using a custom-made photoresistive sensor. Four temporal phases are highlighted in the afferent recording: Stimulus artifact, an artifact due to EMG volume conduction, protraction and retraction phases and a resting state necessary to achieve a vibrissae swept of 10 Hz. (B) Five afferent activity recordings recorded in follows sweep situations: air sweep (control), sweep on wood, sweep on metal, sweep on acrylic and sweep on sandpaper P1000. All activity recordings were obtained at slip-resistance 1. (C) Five afferent activity recordings obtained in different experimental conditions at slip-resistance 2. (D) Idem to C at slip-resistance 4.

Fig. 6 Pairwise comparisons of sweep situations at different slip-resistance levels. (A) Mean and standard deviation of maximum energy components along time obtained from spectrograms of sweep situations at slip-resistance 1. (B) Idem to A at slip-resistance 2. (C) Idem to A at slip-resistance 4.

Fig. 7 Discriminability measures. (A) Mean and standard deviation of maximum energy components along time obtained from spectrograms of two sweep situations at slip-resistance 4 (vibrissa sweep on wood and acrylic surfaces, blue and red shades respectively). (B) Discriminability measures given by information measures (I), Linacre discriminability factor (LDF), Bhattacharyya distance (DB) and univariate standard distance (D). (C) Standardized discriminability factors. All discriminability measures were standardized respect to their mean and standard deviations into resting state.

Fig. 8 Standardized discriminability measures of pairwise comparisons of sweep situations at different slip-resistance levels. (A) Discriminability measures at slip-resistance 1. (B) Idem to A at slip-resistance 2. (C) Idem to A at slip-resistance 4.

Figure1

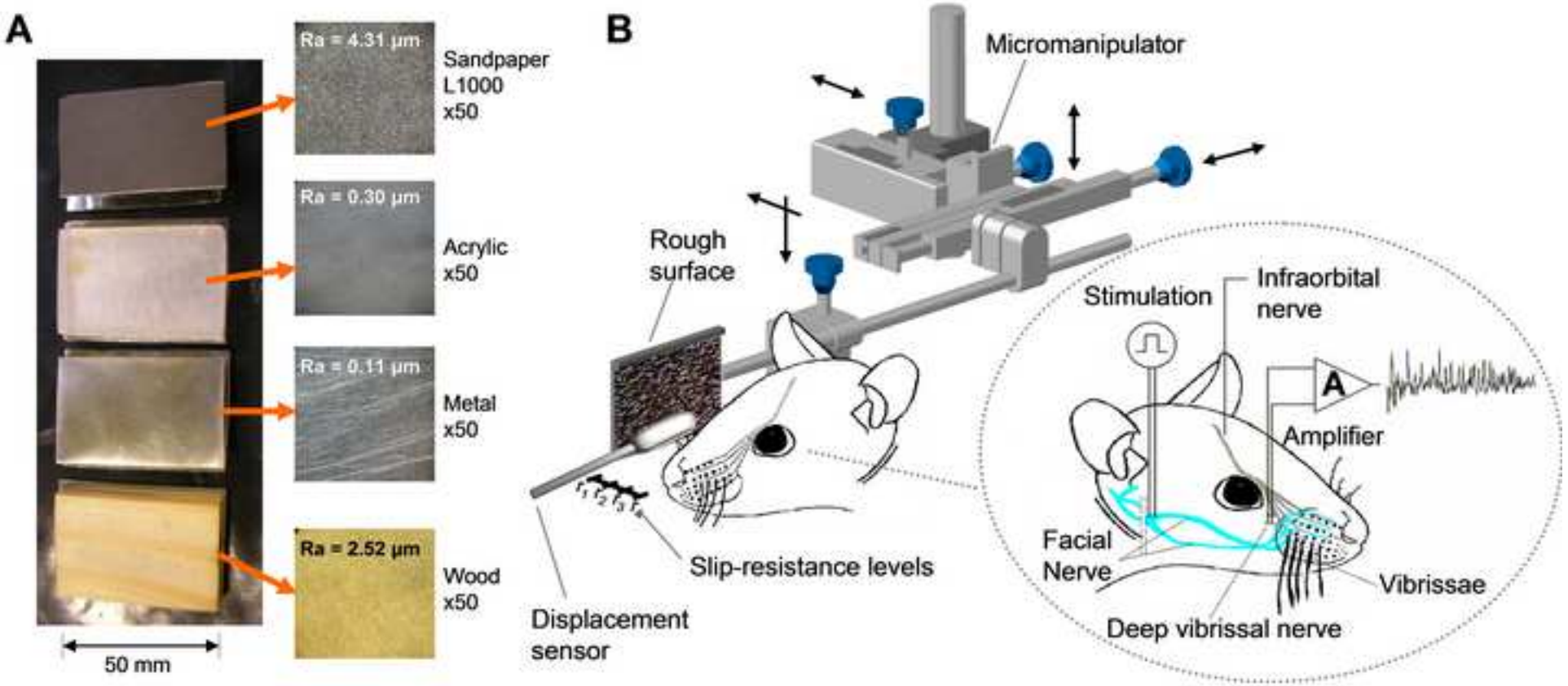
A
Ra = 4.31 µm
Sandpaper
L1000
x50
Ra = 0.30 µm
Acrylic
x50
Ra = 0.11 µm
Metal
x50
Ra = 2.52 µm
Wood
x50
50 mm
B
Micromanipulator
Rough
surface
Stimulation
Infraorbital
nerve
A
Amplifier
Facial
Nerve
Vibrissae
Deep vibrissal nerve
Slip-resistance levels
Displacement
sensor

Figure2

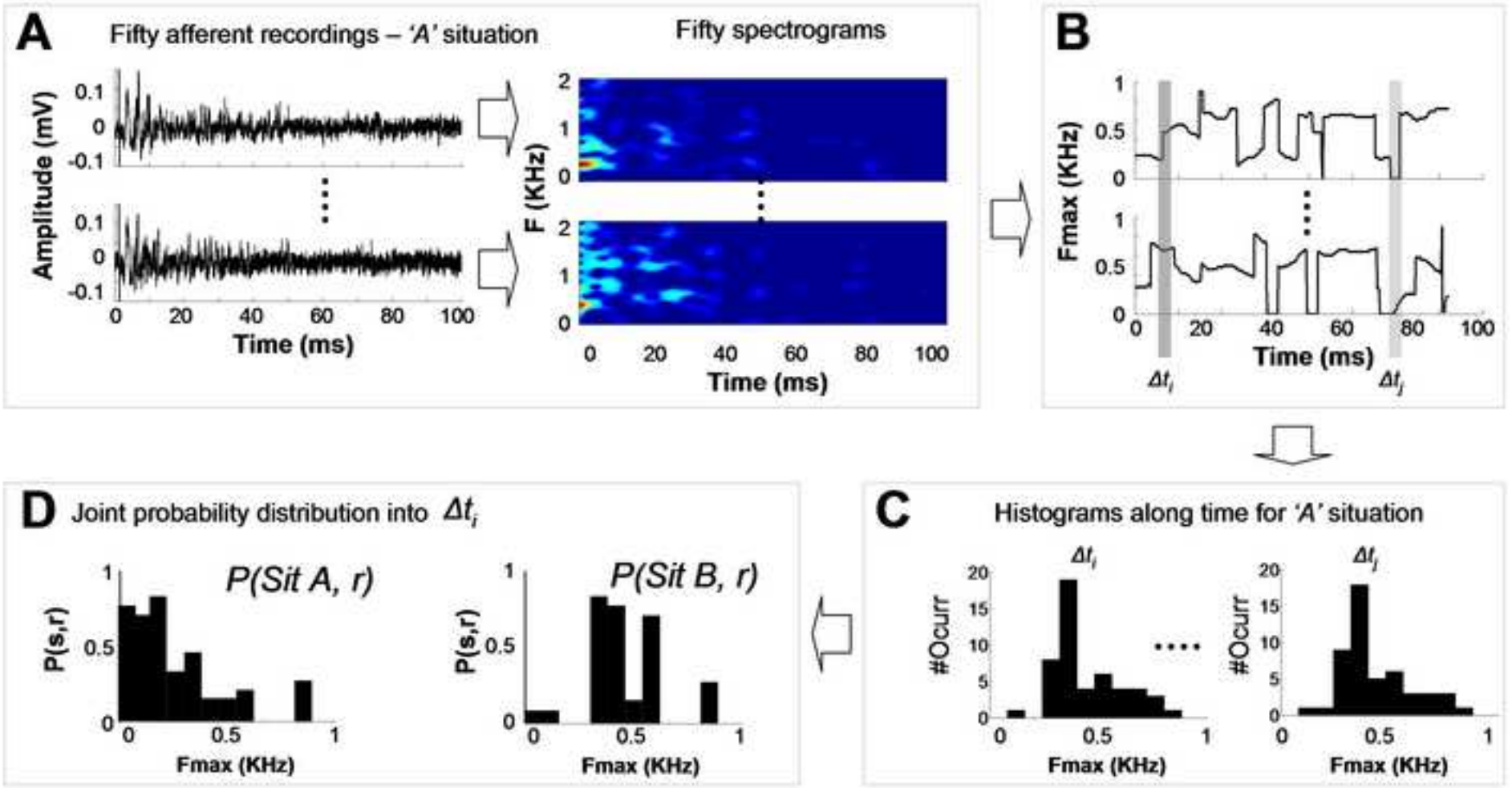
A
Fifty afferent recordings – 'A' situation
Fifty spectrograms
Amplitude (mV)
Time (ms)
F (KHz)
Time (ms)
B
Fmax (KHz)
Time (ms)
Δt_i
Δt_j
C
Histograms along time for 'A' situation
Δt_i
Δt_j
#Ocurr
Fmax (KHz)
D
Joint probability distribution into Δt_i
P(Sit A, r)
P(Sit B, r)
P(s,r)
Fmax (KHz)

Figure3

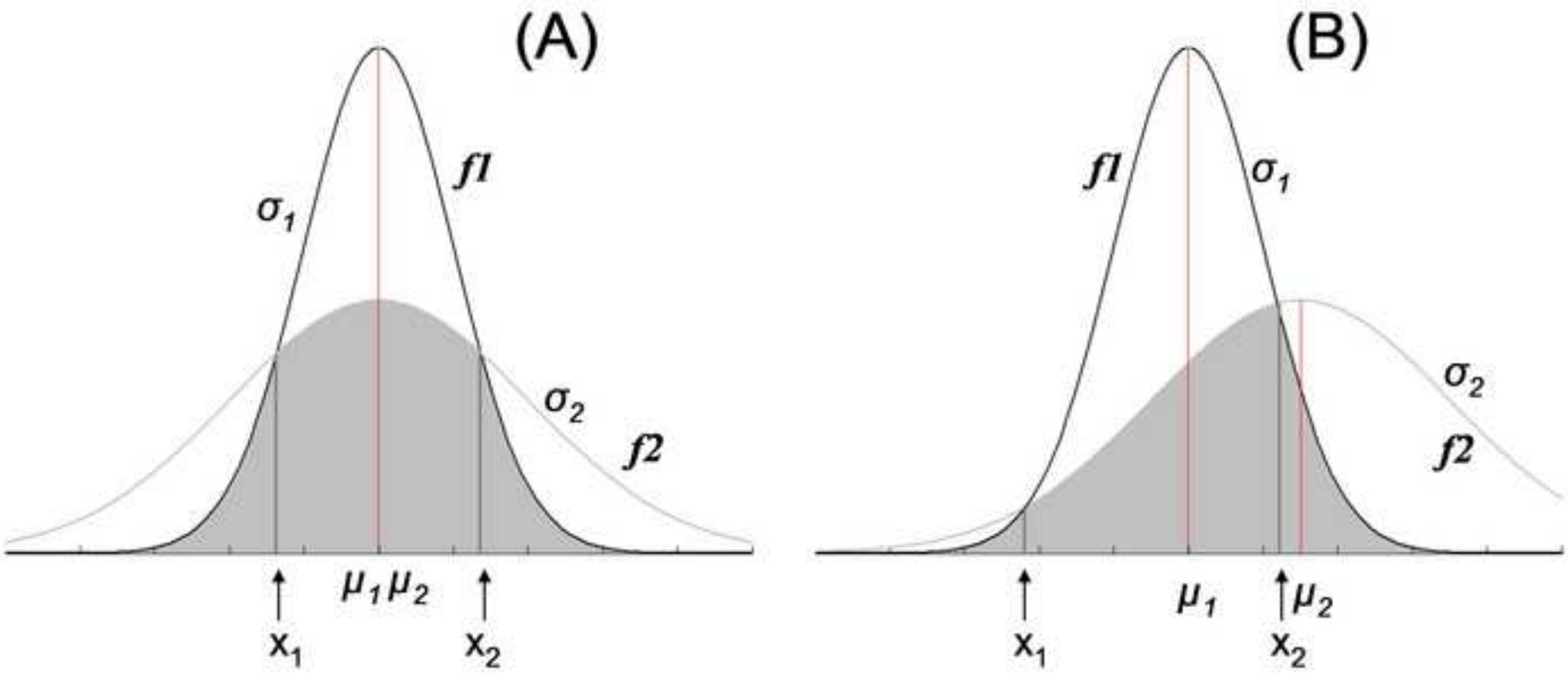

Figure4

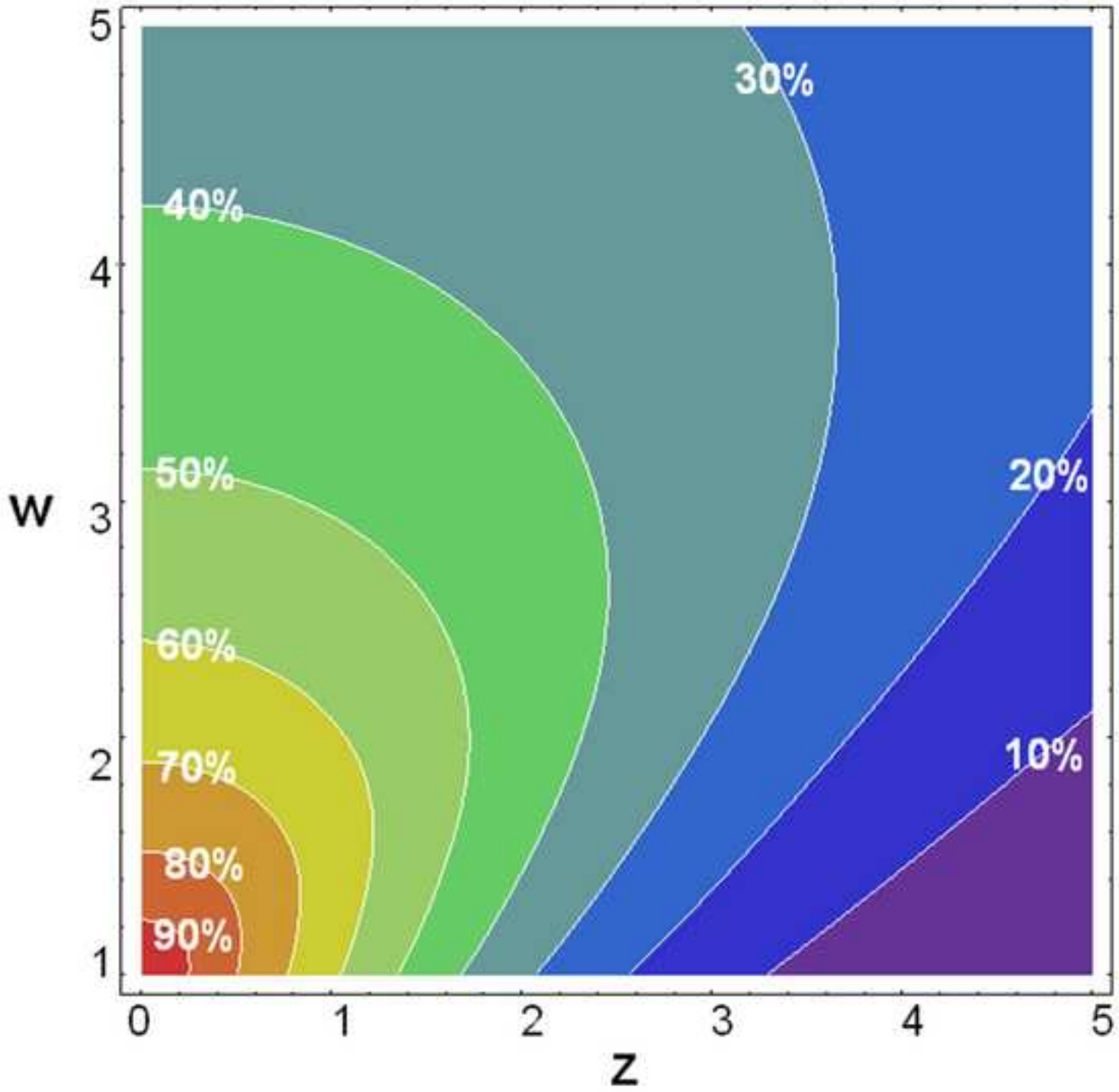

Figure5

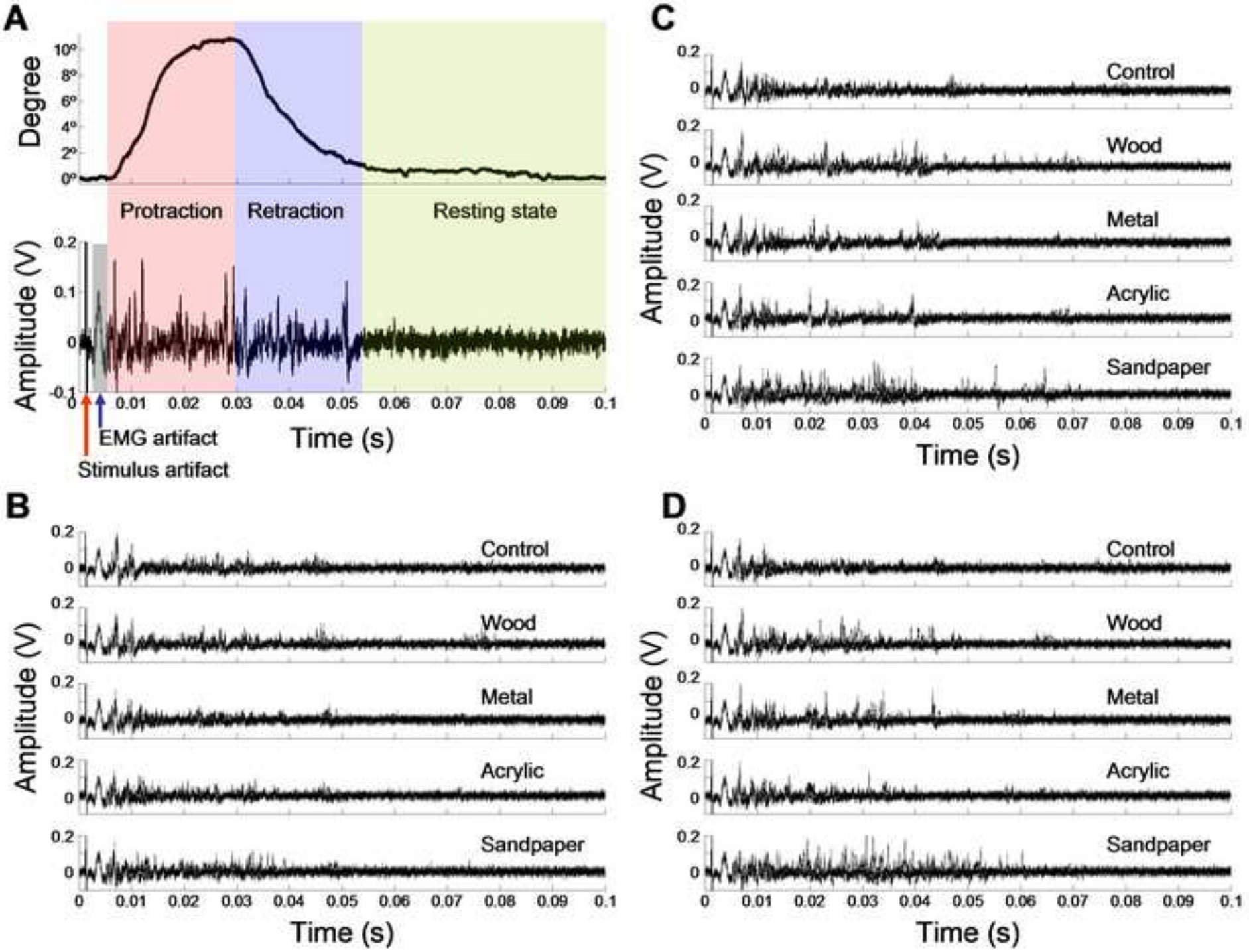
A
Degree
10°
8°
6°
4°
2°
0°
Protraction
Retraction
Resting state
Amplitude (V)
0.2
0.1
0
-0.1
0 0.01 0.02 0.03 0.04 0.05 0.06 0.07 0.08 0.09 0.1
EMG artifact
Stimulus artifact
Time (s)
B
Control
Wood
Metal
Acrylic
Sandpaper
Amplitude (V)
0.2
0
0 0.01 0.02 0.03 0.04 0.05 0.06 0.07 0.08 0.09 0.1
Time (s)
C
Control
Wood
Metal
Acrylic
Sandpaper
Amplitude (V)
0.2
0
0 0.01 0.02 0.03 0.04 0.05 0.06 0.07 0.08 0.09 0.1
Time (s)
D
Control
Wood
Metal
Acrylic
Sandpaper
Amplitude (V)
0.2
0
0 0.01 0.02 0.03 0.04 0.05 0.06 0.07 0.08 0.09 0.1
Time (s)

Figure6

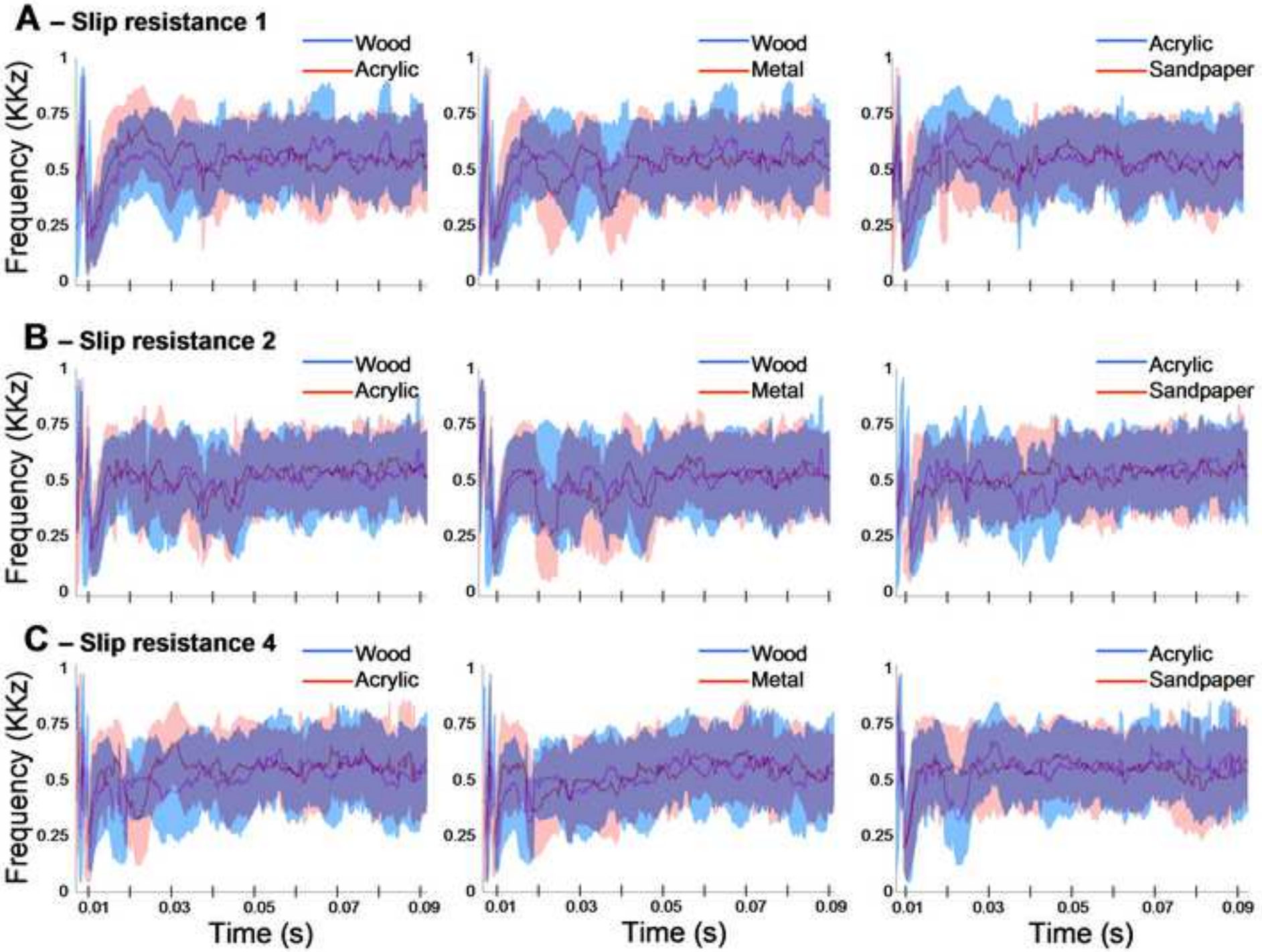
A – Slip resistance 1
Wood
Acrylic
Wood
Metal
Acrylic
Sandpaper
B – Slip resistance 2
Wood
Acrylic
Wood
Metal
Acrylic
Sandpaper
C – Slip resistance 4
Wood
Acrylic
Wood
Metal
Acrylic
Sandpaper
Frequency (KKz)
0
0.25
0.5
0.75
1
0.01
0.03
0.05
0.07
0.09
Time (s)

Figure7

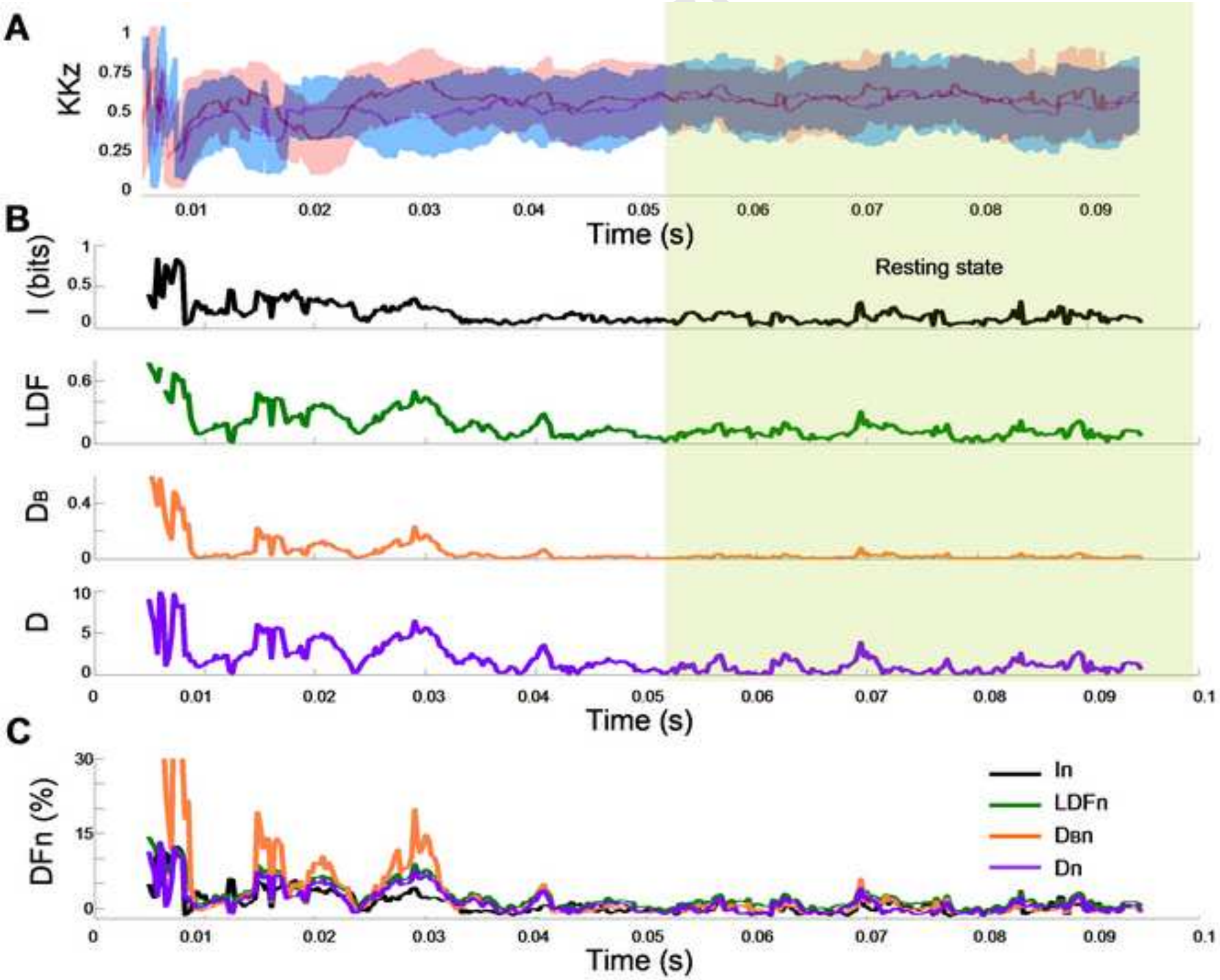
A
KKz
1
0.75
0.5
0.25
0
0.01
0.02
0.03
0.04
0.05
0.06
0.07
0.08
0.09
Time (s)
B
I (bits)
Resting state
LDF
DB
D
10
5
0.1
C
DFn (%)
30
15
In
LDFn
DBn
Dn

Figure8

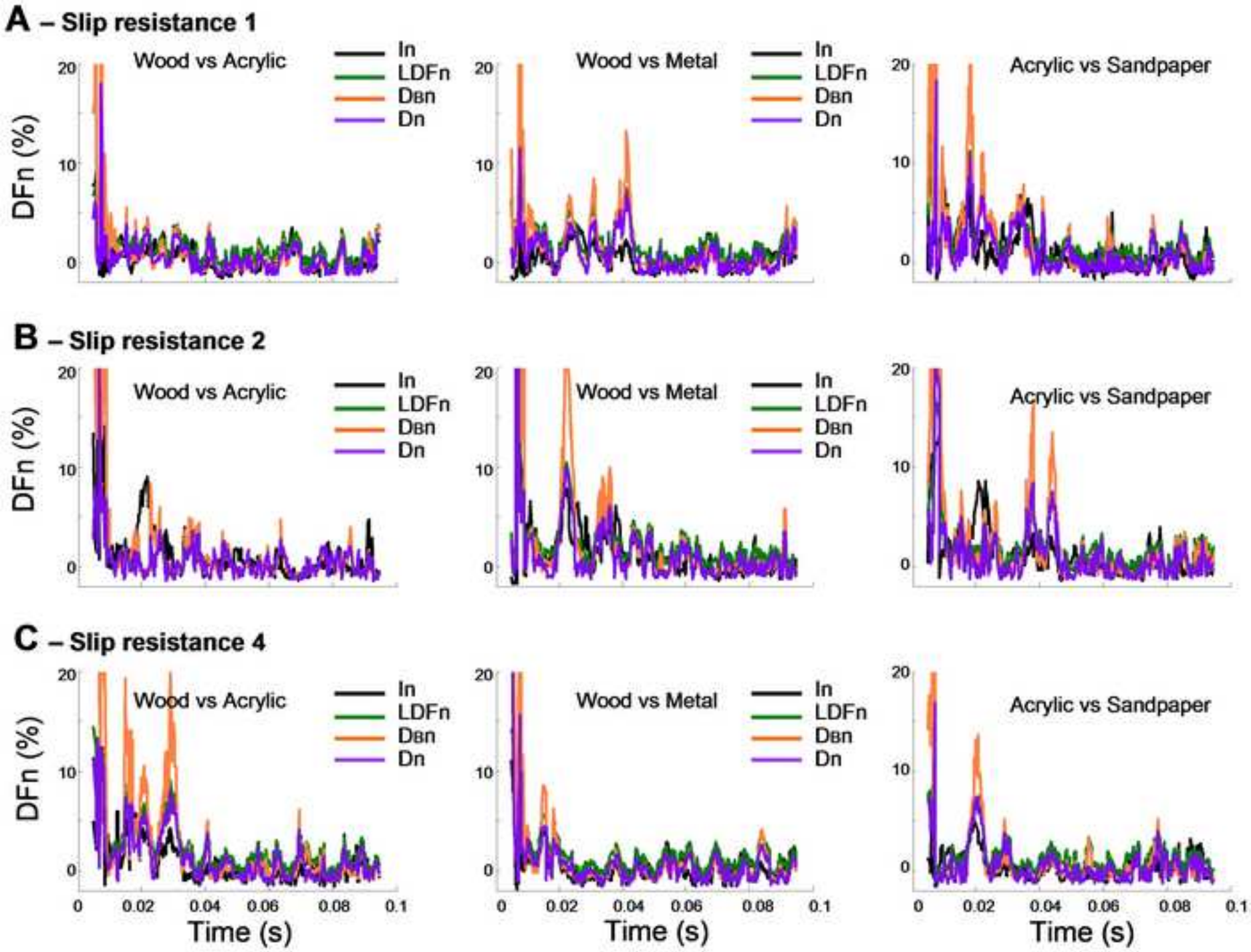
A – Slip resistance 1
B – Slip resistance 2
C – Slip resistance 4
Wood vs Acrylic
Wood vs Metal
Acrylic vs Sandpaper
In
LDFn
DBn
Dn
DFn (%)
Time (s)
0
10
20
0.02
0.04
0.06
0.08
0.1